Secondary structure of the membrane-bound domains of H^+,K^+-ATPase and Ca^{2+}-ATPase, a comparison by FTIR after proteolysis treatment of the native membranes

Vincent Raussens[a], Marc le Maire[b], Jean-Marie Ruysschaert[a], Erik Goormaghtigh[a,*]

[a] *Laboratoire de Chimie-Physique des Macromolécules aux Interfaces, Université Libre de Bruxelles, Campus Plaine CP206/2, B-1050 Brussels, Belgium*

[b] *Section de Biophysique des Protéines et des Membranes, Département de Biologie Cellulaire et Moléculaire, CEA et CNRS URA 2096, Centre d'Etudes de Saclay, 91191 Gif-sur-Yvette Cedex, France*

Received 3 August 1998

Abstract The sarcoplasmic reticulum Ca^{2+}-ATPase and the gastric H^+,K^+-ATPase were cleaved under three different proteolysis conditions. After elimination of the protease and of the cleaved peptides, the vesicles containing the membrane-bound peptides of the ATPases were studied by Fourier transform attenuated total reflection infrared spectroscopy. In the harsher proteolysis conditions, the membrane-associated domain of the Ca^{2+}-ATPase represented about 20% of the protein and was mainly constituted of α-helices. Polarized infrared spectroscopy showed that these α-helices were mainly oriented perpendicular to the membrane. However, only 10–20% of the H^+,K^+-ATPase was cleaved. The remaining, membrane-associated domain of the protein contained about 30% of α-helices and 30% of β-sheet structures. The α-helices adopted a mainly transmembrane orientation. While the data on the Ca^{2+}-ATPase are in general agreement with the current model of the protein, our results indicate that caution must be used in choosing this protein as a general structural model for all P-type ATPases. The protease-resistant, membrane-associated domain of the H^+K^+-ATPase is indeed much larger than predicted and also contained β-sheet structures.

Key words: Gastric H^+,K^+-ATPase; Ca^{2+}-ATPase; Structure; Fourier transform infrared spectroscopy; Proteolysis

1. Introduction

The P-type ATPase family is constituted of more than 100 known proteins. These ATPases are responsible for the transport of different cations across the membranes. Among them, we find the sarcoplasmic reticulum Ca^{2+}-ATPase, the Na^+,K^+-ATPase, the gastric H^+,K^+-ATPase and some H^+-ATPases from plants, yeasts and mushrooms (for recent reviews, see [1,2]). Differences exist between the P-type ATPases. Some are constituted of a single subunit, others are two-subunit complexes (Na^+,K^+- and H^+,K^+-ATPase for example) or even multiple-subunit complexes (as in the case of the Kdp-ATPase) [3]. However, due to homologies in the amino acid sequences, characteristic sequence motifs, and similar hydropathy profiles, they are thought to share a common structural organization. The current models of the P-type ATPases predict a huge cytoplasmic domain representing at least 60% of the protein, a short extracytoplasmic domain and a membrane domain made up of 8–12 transmembrane α-helices. In the N-terminal part of the proteins, the hydropathy profiles and experimental data suggest four transmembrane helices. In the C-terminal part, the profiles are less clear, and the number of predicted transmembrane helices varies from four or six for the Na^+,K^+-ATPase, six for the Ca^{2+}-ATPase [4,5] to eight for the H^+-ATPase of *Neurospora crassa* [6] but recent data fit better with six [7]. The structure at 8 Å resolution of the H^+-ATPase [7] and the Ca^{2+}-ATPase [8] revealed significant differences between these proteins, in particular in the cytoplasmic region in direct contact with the membrane.

Proteolysis by trypsin and proteinase K of the cytoplasmic part of the Ca^{2+}-ATPase from the sarcoplasmic reticulum removes 63% of the protein [9]. This value is in good agreement with the proposed models for this ATPase that predict that the cytoplasmic part of the protein represents ∼70% of the protein [10–12]. Moreover, an analysis by Fourier transform infrared (FTIR) spectroscopy shows the absence of β-sheet structure in the membrane-associated domain after proteolysis [9].

On the other hand, a similar experimental approach applied to the gastric H^+,K^+-ATPase revealed that at most 45% of the protein can be remove by proteolysis [13]. Furthermore, the membrane fraction isolated in this manner contains as much β-sheet as α-helix structure. The discrepancy with the results obtained on the Ca^{2+}-ATPase suggests either a difference in the experimental procedures (incubation time, protease quality, etc.), different protease susceptibility or real structural differences between these two ATPases. Considering the importance of such a question for the understanding of the structure of the P-type ATPases, we have tested, in parallel, different proteolysis conditions on the Ca^{2+}-ATPase and on the H^+,K^+-ATPase. Proteolysis extent and secondary structure of membrane-bound fragments were compared and analyzed by infrared spectroscopy.

2. Materials and methods

2.1. Materials

Proteinase K and trypsin were purchased from Sigma (St. Louis, MO, USA). Deuterium oxide was from Janssen Chimica (Geel, Belgium). All other reagents were of the highest purity grade commercially available.

*Corresponding author. Fax: (32) (2) 650 53 82.

Abbreviations: ATR-FTIR, attenuated total reflection Fourier transform infrared; PMSF, phenylmethylsulfonyl fluoride; SDS-PAGE, sodium dodecyl sulfate polyacrylamide gel electrophoresis; SR, sarcoplasmic reticulum

0014-5793/98/$19.00
PII: S0014-5793(98)01225-3

2.2. Ca^{2+}-ATPase purification

Tight SR vesicles were prepared from rabbit skeletal muscle as described [14,15]. Purified ATPase preparations were obtained by extraction with a low concentration of deoxycholate [16].

2.3. H^+,K^+-ATPase purification

Tubulovesicles, containing the gastric H^+,K^+-ATPase, were isolated from hog gastric fundus by differential centrifugation as described [17]. They were further purified from the microsomal fractions by centrifugation on a sucrose discontinuous density gradient at $100\,000 \times g$ overnight. The material collected at the 8–30% sucrose interface is referred to as the tubulovesicles. A main band at 95 kDa corresponding to the α subunit was visible after Tricine SDS-PAGE analysis of 6 μg on a mini-protean II (Bio-Rad) [13]. Other SDS-PAGE conditions revealed in addition the presence of the β subunit [18].

2.4. Proteolysis

We used three different conditions for the proteolytic degradation of the water-exposed domains of both ATPases.

The first condition, referred to as condition 1 further in the text, had been used previously by Juul et al. [19]. Briefly, the ATPase was digested in the presence of proteinase K (protease/protein ratio of 1/33 (w/w)) during 80 min at 20°C. Proteolysis was stopped by addition of PMSF (0.5 mM final). The soluble cleaved peptides and the protease were eliminated by centrifugation and discarding of the supernatant.

The second condition, referred to as condition 2 in the text, was the one previously described by Corbalan-Garcia et al. [9]. The ATPase was first digested by trypsin (protease/protein ratio of 1/4 (w/w)) during 30 min at 35°C. Proteolysis was stopped by addition of soybean trypsin inhibitor (Sigma). The soluble cleaved peptides and the protease were eliminated by centrifugation and discarding of the supernatant. A second digestion with proteinase K was made (protease/protein ratio of 1/16 (w/w)) during 30 min at 25°C. After addition of PMSF to stop the reaction, the soluble cleaved peptides and the protease were eliminated by centrifugation and discarding of the supernatant.

The third condition, referred to as condition 3 in the text, had been used previously on the H^+,K^+-ATPase [13]. The ATPase was digested by proteinase K (protease/protein ratio of 1/2 (w/w)) during 1 h at 37°C. Proteolysis was stopped by PMSF (6 mM final). The soluble cleaved peptides and the protease were eliminated by centrifugation and discarding of the supernatant.

2.5. FTIR spectroscopy

Attenuated total reflection (ATR) FTIR spectra were recorded on a Perkin-Elmer infrared spectrophotometer 1720X equipped with a liquid nitrogen-cooled MCT detector. The internal reflection element was a germanium ATR plate ($50 \times 20 \times 2$ mm) with an aperture angle of 45° yielding 25 internal reflections. Sixty-four scans were averaged for each spectrum. Spectra were recorded at a nominal resolution of 4 cm^{-1}. The spectrophotometer was continuously purged with air dried on a silicagel column (5×130 cm) at a flow rate of 7 l/min. Every four scans, reference spectra of a clean germanium plate were automatically recorded by a sample shuttle accessory.

2.6. Preparation of the samples

Thin films were obtained as described by Fringeli and Günthard [20] by slowly evaporating 40–100 μl of the membrane suspensions under a N_2 stream on one side of a germanium plate. This results in the formation of oriented multilayers at the surface of the plate. The ATR plate was then sealed in a sample holder and rehydrated by flushing D_2O-saturated N_2 at room temperature.

2.7. Lipid/ATPase ratio

The lipid/protein (w/w) ratio is related to the $\nu(C=O)_{lipid}/\nu(C=O)_{protein}$ absorption bands ratio in the FTIR spectra. The ATPase/lipid ratio after hydrolysis was estimated from the ratio of the protein absorption peak (amide I (1600–1700 cm^{-1})) with respect to the lipid (C=O) absorption peak (1700–1800 cm^{-1}) as established in [21] and used recently in a similar situation [13].

2.8. Secondary structure determination

Fourier self-deconvolution was applied to narrow the different components of the amide. Self-deconvolution was carried out using a Lorentzian line shape for the deconvolution and a Gaussian line shape for the apodization. The quantification of the area of the different components of amide I revealed by the self-deconvolution was obtained as previously described [21].

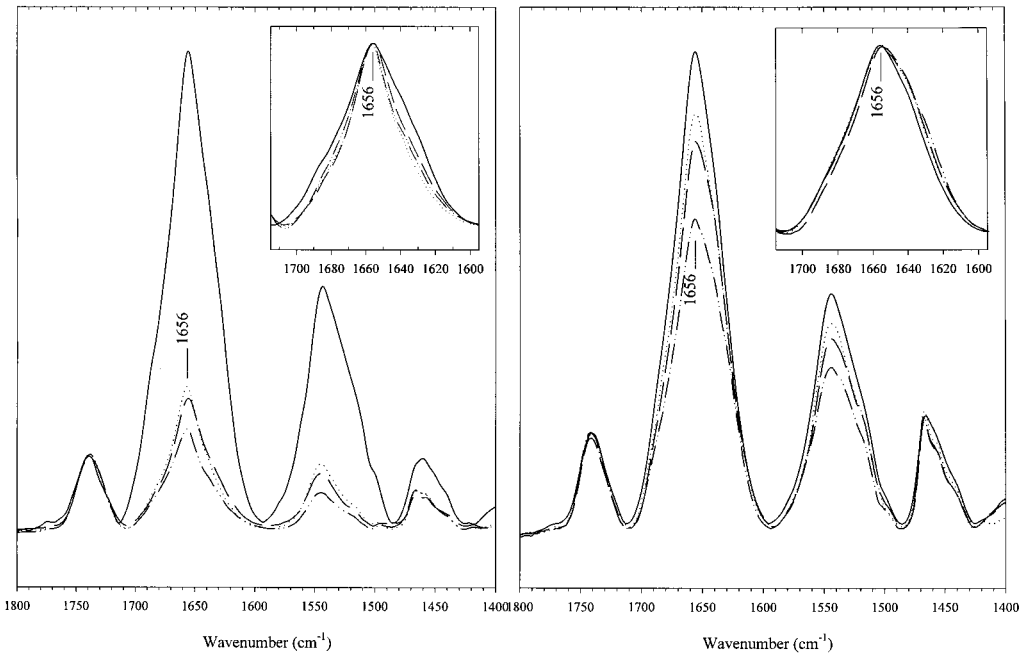

Fig. 1. A: Superimposition of the native Ca^{2+}-ATPase (solid line) and the membrane-bound Ca^{2+}-ATPase peptides obtained after proteolysis by proteinase K (condition 1: dotted line, condition 2: dashed line, and condition 3: dash dot dot line) spectra. B: Superimposition of the native H^+,K^+-ATPase (solid line) and the membrane-bound H^+,K^+-ATPase peptides obtained after proteolysis by proteinase K digested (condition 1: dotted line, condition 2: dashed line, and condition 3: dash dot dot line) spectra. The spectra have been normalized to the same lipid $\nu(C=O)$ ($\sim$1740 cm^{-1}) intensity. The insets display the amide I region of the different spectra. In order to compare the shape of the amide, amide I has been rescaled to the same intensity in all cases.

Table 1
Percentage of proteolysis determined by IR spectroscopy (in parentheses: number of amino acid residues remaining associated with the membrane after proteolysis) for the different proteolysis conditions (see text)

Proteolysis condition:	1	2	3
Ca^{2+}-ATPase (997 aa)	76% (239 aa)	77% (229 aa)	83% (169 aa)
H^+,K^+-ATPase (1324 aa)	11% (1178 aa)	12% (1165 aa)	23% (887 aa)

The number of amino acids indicated for the H^+,K^+-ATPase includes both the α and β subunits [13].

2.9. Orientation of the secondary structures

The determination of molecular orientations by infrared ATR spectroscopy was performed as described [22]. When orientation was to be evaluated, additional spectra were recorded with perpendicular and parallel polarized incident light. The dichroism spectrum was computed by subtracting the perpendicular polarized spectrum from the parallel polarized spectrum taking into account the difference in the relative power of the evanescent field for each polarization as described before [23]. An upward deviation on the dichroism spectrum indicates a dipole oriented close to normal to the ATR plate. Conversely, a downward deviation on the dichroism spectrum indicates a dipole oriented closer to the plane of the ATR plate.

3. Results

3.1. Proteolysis extent

During this work, we used three different proteolysis conditions (referred to as conditions 1, 2, and 3; see Section 2.4) in parallel on both Ca^{2+}-ATPase and H^+,K^+-ATPase. Condition 1 was the mildest one, and has been previously used on the Ca^{2+}-ATPase [19]. Two other conditions had been previously used for studies by IR spectroscopy but on different ATPases and with contradictory results ([9,13] for the Ca^{2+}-ATPase and H^+,K^+-ATPase, respectively). Fig. 1 presents the spectra of the Ca^{2+}-ATPase (panel A) and H^+,K^+-ATPase (panel B) vesicles before and after proteolysis in the different conditions described (see Section 2.4). The relative decrease of the amide I intensity (1700–1600 cm^{-1}) is proportional to the number of peptide bonds present in the sample. Fig. 1 indicates that this decrease is much more important in the case of the Ca^{2+}-ATPase than in the case of the H^+,K^+-ATPase for all the proteolysis conditions. The percentages of removal of proteinaceous materials from the lipid vesicles have been evaluated from the change of the amide I/$\nu(C=O)_{ester}$ ratio upon proteolysis (Table 1). Clearly, susceptibility to proteolysis of the two ATPases is significantly different.

3.2. Secondary structure of the ATPases and of their protease resistant membrane-bound domains

In a first step, we compared the spectra of each native ATPase with the spectra of the membrane-attached fraction obtained after the various digestion conditions described in Section 2.4. In the case of the H^+,K^+-ATPase and for all the proteolysis conditions used here, the shape of the amide I peak was not significantly affected by the proteolysis (Fig. 1B, inset). Qualitatively, these results suggest a similar content in α-helix and β-sheet for the extramembrane and the membrane-associated domains of the gastric ATPase. In contrast, proteolysis of the Ca^{2+}-ATPase in any of the conditions tested resulted in a narrowing of the amide I peak with a maximum

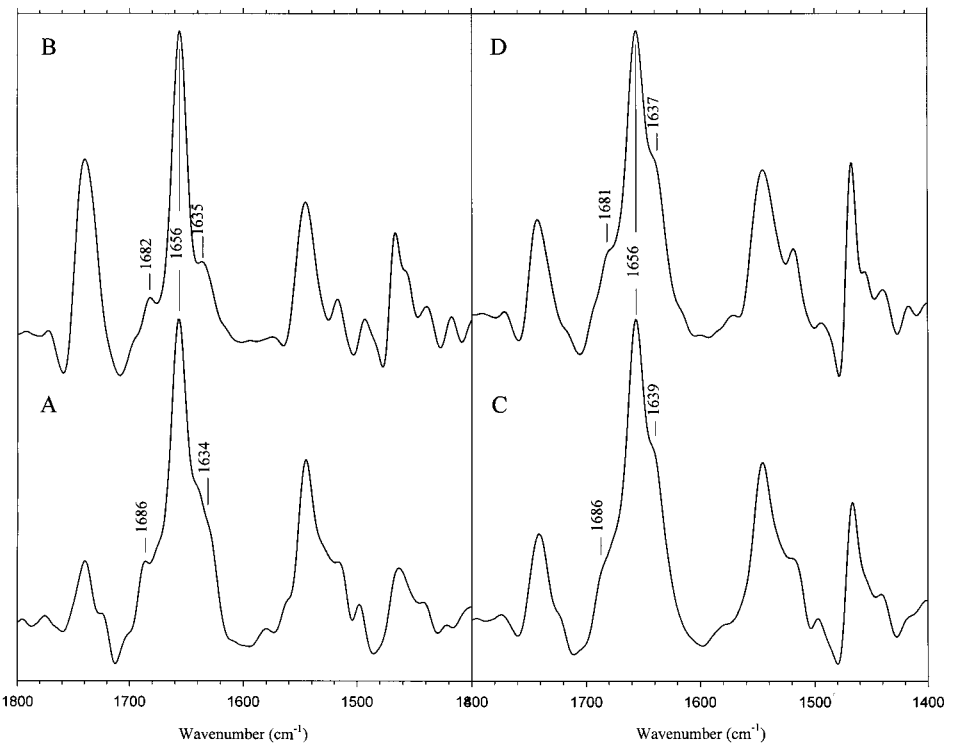

Fig. 2. Deconvolved spectra of the native Ca^{2+}-ATPase (A), the digested Ca^{2+}-ATPase (B), the native H^+,K^+-ATPase (C), and the digested H^+,K^+-ATPase (D). The ATPases have been proteolysed with proteinase K in condition 1 (see text).

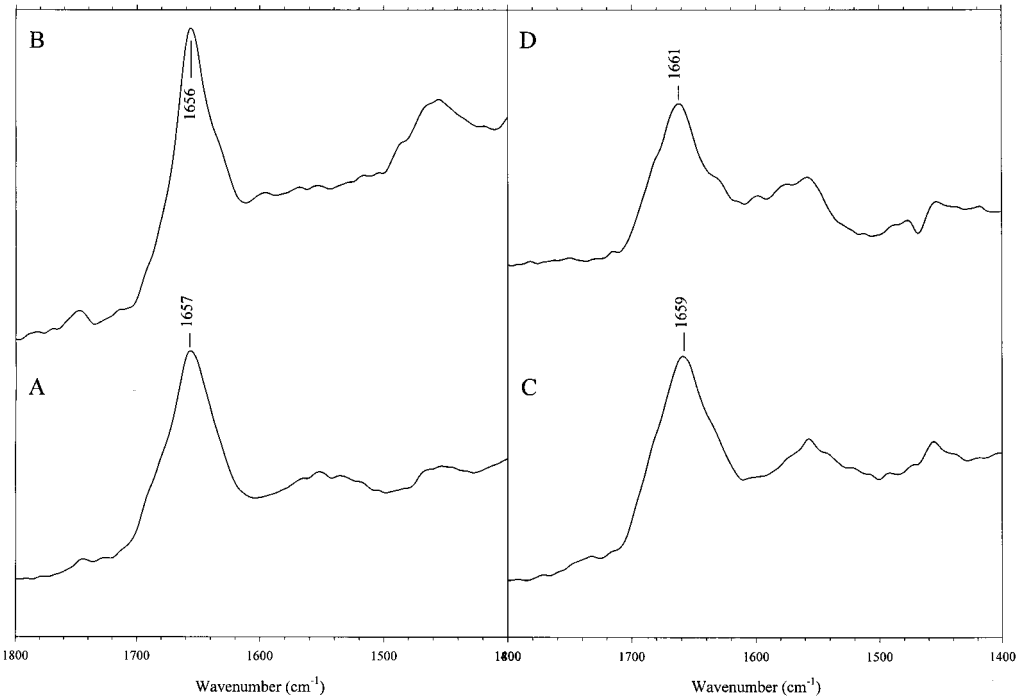

Fig. 3. Dichroic spectra of the native Ca^{2+}-ATPase (A), the digested Ca^{2+}-ATPase (B), the native H^+,K^+-ATPase (C), and the digested H^+,K^+-ATPase (D). The ATPases have been proteolysed with proteinase K in condition 1 (see text). The spectra have been rescaled to the same scale.

located at 1656 cm^{-1} (Fig. 1A, inset). These helices are present in the membrane-associated part of the Ca^{2+}-ATPase. In order to better visualize the different components of the amide I bands, the different spectra of Fig. 1 were deconvolved (Fig. 2). The left panel of Fig. 2 shows the deconvolved spectra of the Ca^{2+}-ATPase before (Fig. 2A) and after proteolysis (Fig. 2B) (condition 1). Two major components located at 1656 and 1634 cm^{-1} appear in the native Ca^{2+}-ATPase spectrum. These two components can be respectively assigned to α-helix and β-sheet structures [24]. After proteolysis (Fig. 2B), the intensity of the β-sheet component at 1635 cm^{-1} decreases significantly with respect to the α-helix component at 1656 cm^{-1}. The deconvolved spectra of the gastric H^+,K^+-ATPase appear in the right panel of Fig. 2. As for the Ca^{2+}-ATPase, two major amide I components are located at 1656 and 1639 cm^{-1}, respectively assigned to α-helix and β-sheet structures. However, in the case of the H^+,K^+-ATPase, they keep about the same relative intensity before (Fig. 2C) and after proteolysis (Fig. 2D) indicating a similar α-helix and β-sheet content before and after proteolysis.

A quantitative analysis by Fourier transform deconvolution and least square curve fitting [21] of the amide I peaks of spectra, recorded after deuteration during 2 h, allowed us to calculate the different secondary structure contents (Table 2). As qualitatively observed previously, an important increase of the α-helix content (from 48% to 59–64%) in the membrane part of the Ca^{2+}-ATPase and a simultaneous decrease in the β-sheet content (from 24% to 12–17%) was found. No significant change of the α-helix (30–35%) and β-sheet (30–35%) content was observed in the case of the H^+,K^+-ATPase.

3.3. Orientation of the secondary structures

In order to define the orientation of the proteins with regard to the membrane plane, we recorded spectra with parallel or perpendicular polarized light (see Section 2.9). The dichroic spectra of the Ca^{2+}-ATPases, native or proteolysed under the different experimental conditions, show a positive deviation at $\sim$1656 cm^{-1}, a spectral region characteristic of α-helical structures. The results obtained for proteolysis with condition 1 are presented in Fig. 3B. The dichroic spectra of the H^+,K^+-

Table 2
Percentages of secondary structures determined by deconvolution and least square fitting of the amide I peak for the native ATPases and ATPase membrane-bound peptides after proteolysis in conditions 1, 2, and 3 (for conditions see text)

		α-helix (%)	β-sheet (%)	turn (%)	random (%)
Ca^{2+}-ATPase	native (997 aa)	48 (479)	24 (239)	13 (130)	14 (140)
	Cond. 1 (239 aa)	64 (153)	12 (29)	8 (19)	16 (38)
	Cond. 2 (229 aa)	59 (135)	14 (32)	7 (16)	20 (46)
	Cond. 3 (169 aa)	64 (108)	17 (29)	5 (8)	13 (22)
H^+,K^+-ATPase	native (1324 aa)	32 (424)	31 (410)	16 (212)	20 (265)
	Cond. 1 (1178 aa)	34 (400)	34 (400)	18 (212)	14 (165)
	Cond. 2 (1165 aa)	29 (338)	28 (326)	28 (326)	16 (186)
	Cond. 3 (887 aa)	37 (328)	38 (337)	24 (213)	0 (0)

In parentheses, the number of amino acids corresponding to the different percentages.

ATPases, native or proteolysed under the different experimental conditions, show a positive deviation at ~1660 cm^{-1}, in the same spectral region characteristic of α-helical structures. The results obtained for proteolysis with condition 1 are presented in Fig. 3D. The amide I dipole in an α-helix is close to a parallel to the helix axis, so the positive deviation indicates a helix orientation mainly perpendicular to the plane of the membrane. Such an orientation is expected for transmembrane helices, and is clearly observed for both ATPases.

4. Discussion and conclusions

The Ca^{2+}-ATPase is one of the most studied and best characterized P-type ATPases. The proposed models for this ATPase, based on predictive methods [2,10,25], on experimental data [5,26,27] including two-dimensional crystal analysis [8,12,28,29], agree with an insertion of the protein in the lipid membrane with about 10 transmembrane α-helices, a large cytoplasmic domain (~70%) and a small extracytoplasmic one.

The experiments carried out during this work on the Ca^{2+}-ATPase are in agreement with such a model. A cytoplasmic domain accounting for at least 70% of the protein (Table 1), a membrane domain essentially in an α-helix conformation (Table 2) and the orientation of these helices mainly perpendicular to the plane of the membrane (Fig. 3) are all results confirming the model.

The proposed models for the other P-type ATPases are mainly derived from hydropathy index profiles and by comparison with the Ca^{2+}-ATPase model. The proteolysis experiments on the gastric H^+,K^+-ATPase are not entirely in agreement with such models. First the membrane-bound, proteolysis-insensitive domain of the gastric ATPase seems to be much more important than for the Ca^{2+}-ATPase. We have shown previously that in drastic proteolysis conditions (protease/protein ratio > 1 with sequential additions of proteases during the proteolysis, 24 h of proteolysis at 37°C), the protected part of the ATPase remaining attached to the membrane represents 45–50% of the protein [13]. Furthermore, the membrane-bound, protease-insensitive domain of the gastric ATPase contains not only α-helices, as in the case of Ca^{2+}-ATPase, but also β-sheet structures

The proteolysis experiments on the Ca^{2+}-ATPase and on the H^+,K^+-ATPase have been carried out here in parallel (same timing, same temperature, same proteases, etc.), and the results have been analyzed according to the same procedure. We can therefore be rather confident that the differences observed during this work are due to real structural differences between the two ATPases. A weaker proteolytic efficiency of proteinase K on the H^+,K^+-ATPase, especially in the rather drastic conditions used here (and also previously [13]) seems to be highly unlikely. Since even in the presence of both trypsin and proteinase K in association the percentage of proteolysis does not increase, this rules out a possible specificity of proteinase K for selected amino acids.

At this point, two possibilities remain: (1) the gastric H^+,K^+-ATPase contains a membrane-associated domain which contains β-sheet structures, resistant to proteolysis and much larger than the Ca^{2+}-ATPase one; (2) the structure of several segments protruding from the membrane is such that they are resistant to both trypsin and proteinase K, even in the harshest conditions. Other experiments reported in the literature suggest that the behavior of the H^+,K^+-ATPase is not unique. Proteolysis experiments on the *N. crassa* H^+-ATPase indicated that the membrane domain represents 48% of the protein [23]. Chemical labeling experiments suggested that models of the Na^+,K^+-ATPase based on hydrophobicity of the amino acids sequence underestimate the amount of protein inserted in the lipid membrane [30]. Moreover, extensive proteolysis experiments of the Na^+,K^+-ATPase showed that around 50% of the protein remains associated with the membrane after digestion [31]. Also low resolution X-ray diffraction of Na^+,K^+-ATPase crystals showed that its membrane part should represent 30–40% of the total mass of the protein [32,33]. In conclusion, the present data suggest that building structural models of any P-type ATPase based only on the knowledge of the Ca^{2+}-ATPase structure must be considered with caution.

Acknowledgements: E.G. is Senior Research Associate and V.R. is senior research assistant of the National Fund for Scientific Research (Belgium). We thank the Action de la Recherche Concertée (Belgium) and the CEA and CNRS (France) and the Association Française contre les Myopathies for their financial support.

References

[1] Lutsenko, S. and Kaplan, J.H. (1996) Trends Biochem. Sci. 21, 237–241.
[2] Møller, J., Juul, B. and le Maire, M. (1996) Biochim. Biophys. Acta 1286, 1–51.
[3] Altendorf, K., Siebers, A. and Epstein, W. (1992) Ann. NY Acad. Sci. 671, 228–243.
[4] MacLennan, D., Clarke, D., Loo, T. and Skerjanc, I. (1992) Acta Physiol. Scand. 146, 141–150.
[5] le Maire, M. (1995) J. Biol. Chem. 270, 20123–20134.
[6] Scarborough, G.A. (1992) Mol. Cell. Biochem. 114, 49–56.
[7] Auer, M., Scarborough, G.A. and Kühlbrandt, W. (1998) Nature 392, 840–843.
[8] Zhang, P., Toyoshima, C., Yonekura, K., Greens, N.M. and Stokes, D.L. (1998) Nature 392, 835–839.
[9] Corbalan-Garcia, S., Teruel, J., Villalain, J. and Gomez-Fernandez, J. (1994) Biochemistry 33, 8247–8254.
[10] Brandl, C., Green, N., Korczak, B. and MacLennan, R. (1986) Cell 44, 597–607.
[11] Clarke, D., Loo, T., Inesi, G. and MacLennan, D. (1989) Nature 339, 476–478.
[12] Stokes, D. and Green, N.M. (1990) Biochem. Soc. Trans. 18, 841–843.
[13] Raussens, V., Ruysschaert, J.M. and Goormaghtigh, E. (1997) J. Biol. Chem. 272, 262–270.
[14] de Meis, L. and Hasselbach, W. (1971) J. Biol. Chem. 246, 4759–4763.
[15] Champeil, P., Guillain, F., Vénien, C. and Gingold, M.P. (1985) Biochemistry 24, 69–81.
[16] Meissner, G., Conner, G. and Fleischer, S. (1973) Biochim. Biophys. Acta 298, 246–269.
[17] Soumarmon, A., Abastado, M., Bonfils, S. and Lewin, M. (1980) J. Biol. Chem. 255, 11682–11687.
[18] Soulié, S., Denoroy, L., Le Caer, J.-P., Hamasaki, N., Groves, J.D. and le Maire, M. (1998) J. Biochem. 124 (in press).
[19] Juul, B., Turc, H., Durand, M., Gomez de Gracia, A., Denoroy, L., Møller, J., Champeil, P. and le Maire, M. (1995) J. Biol. Chem. 270, 20123–20134.
[20] Fringeli, U. and Günthard, H. (1981) in: Membrane Spectroscopy (Grell, E., Ed.), pp. 270–332, Springer Verlag, Berlin.
[21] Goormaghtigh, E., Cabiaux, V. and Ruysschaert, J.-M. (1990) Eur. J. Biochem. 193, 409–420.
[22] Goormaghtigh, E. and Ruysschaert, J.-M. (1990) in: Molecular Description of Biological Membrane Components by Computer Aided Conformational Analysis (Brasseur, R., Ed.), pp. 285–329, CRC Press, Boca Raton FL.

[23] Vigneron, L., Ruysschaert, J.M. and Goormaghtigh, E. (1995) J. Biol. Chem. 270, 17685–17696.
[24] Goormaghtigh, E., Cabiaux, V. and Ruysschaert, J.-M. (1994) Subcell. Biochem. 23, 405–450.
[25] Green, N. (1989) Biochem. Soc. Trans. 17, 972–974.
[26] MacLennan, D., Brandl, C., Korczak, B. and Green, N. (1985) Nature 316, 696–700.
[27] Andersen, J. and Vilsen, B. (1992) Acta Physiol. Scand. 146, 151–159.
[28] Taylor, K., Dux, L. and Martonosi, A. (1986) J. Mol. Biol. 187, 417–427.
[29] Stokes, D., Taylor, W. and Green, N. (1994) FEBS Lett. 346, 32–38.
[30] Sweadner, K. and Arystarkhova, E. (1992) Ann. NY Acad. Sci. 671, 217–227.
[31] Capasso, J., Hoving, S., Tal, D., Goldshleger, R. and Karlish, S. (1992) J. Biol. Chem. 267, 1150–1158.
[32] Herbert, H., Skriver, E. and Maunsbach, A. (1985) FEBS Lett. 187, 182–187.
[33] Maunsbach, A., Skriver, E., Soderholm, M. and Hebert, H. (1988) Prog. Clin. Biol. Res. 268, 39–56.